

Effect of gluon condensate on holographic Schwinger effect

Zi-qiang Zhang,^{1,*} Xiangrong Zhu,^{2,†} and De-fu Hou^{3,‡}

¹*School of Mathematics and Physics, China University of Geosciences, Wuhan 430074, China*

²*School of Science, Huzhou University, Huzhou 313000, China*

³*Central China Normal University, Wuhan 430079, China*

We perform the potential analysis in holographic Schwinger effect in a deformed anti-de Sitter (AdS) background with backreaction due to the gluon condensate. We determine the potential by analyzing the classical string action attaching on a probe D3-brane sitting at an intermediate position in the bulk AdS space. It is found that the inclusion of the gluon condensate reduces the production rate, reverse to the effect of the temperature. Also, we evaluate the critical electric field by Dirac-Born-Infeld (DBI) action.

PACS numbers: 11.25.Tq, 11.15.Tk, 11.25-w

I. INTRODUCTION

It is generally accepted that vacuum in quantum field theory (QFT) is not actually barren. Rather, it contains lots of virtual particles and antiparticles due to quantum fluctuations. For instance, in the vacuum of quantum electrodynamics (QED), virtual electron-positron pairs are supposed to be momentarily created and annihilated. Moreover, these virtual particles could be materialized and become real particles in a strong electric-field. This non-perturbative phenomenon is known as the Schwinger effect. The production rate Γ (per unit time and volume) has been evaluated by Schwinger for the case of weak-coupling and weak-field in 1951 [1]

$$\Gamma \sim \exp\left(\frac{-\pi m^2}{eE}\right), \quad (1)$$

where E , m and e are an external electric-field, an electron mass and an elementary electric charge, respectively. Thirty one years later, Affleck-Alvarez-Manton (AAM) generalized it to the case of arbitrary-coupling and weak-field [2]

$$\Gamma \sim \exp\left(\frac{-\pi m^2}{eE} + \frac{e^2}{4}\right), \quad (2)$$

From the above formulas of Γ , one finds there is no critical field in the Schwinger case. While in the AAM case, there is a critical field at $eE_c = (4\pi/e^2)m^2 \simeq 137m^2$, but it is far beyond the weak-field condition $eE \ll m^2$. Thus, it seems that one could not get the critical field under the weak-field condition.

Actually, the Schwinger effect is not confined to QED but ubiquitous for QFT coupled to an U(1) gauge field. However, it remains difficult to tackle this issue with the standard method in QFT. A possible way is to use the AdS/CFT correspondence [3–5] by realizing QFT (or rather confining gauge theories) with appropriate D-brane set-up. In 2011, Semenoff and Zarembo proposed [6] that the Schwinger effect could be modeled in the higgsed $\mathcal{N} = 4$ supersymmetric Yang-Mills (SYM) theory. Specifically, a $\mathcal{N} = 4$ SYM theory system coupled with an U(1) gauge field can be realized by breaking the gauge group from $SU(N+1)$ to $SU(N) \times U(1)$ via the Higgs mechanism. In this approach, the production rate and the critical electric field (at large N and large 't Hooft coupling λ) are evaluated as

$$\Gamma \sim \exp\left[-\frac{\sqrt{\lambda}}{2}\left(\sqrt{\frac{E_c}{E}} - \sqrt{\frac{E}{E_c}}\right)^2\right], \quad E_c = \frac{2\pi m^2}{\sqrt{\lambda}}, \quad (3)$$

interestingly, the resulting critical field is completely consistent with the DBI result. Subsequently, there are many attempts to address the holographic Schwinger in this direction. For instance, the potential analysis in holographic

*Electronic address: zhangzq@cug.edu.cn

†Electronic address: xrongzhu@zjhu.edu.cn

‡Electronic address: houdf@mail.ccnu.edu.cn

Schwinger effect has been investigated in various backgrounds [7–13]. The holographic Schwinger effect and negative differential conductivity have been discussed in [14]. The holographic Schwinger effect with constant electric and magnetic fields was considered in [15, 16]. For a study of this quantity in de Sitter spacetime, see [17]. Moreover, the holographic Schwinger effect has been analyzed from the imaginary part of a probe brane action [18–21]. For a recent review on this topic, see [22].

The aim of this paper is to study the effect of the gluon condensate on the (holographic) Schwinger effect. The gluon condensate was proposed in [23] as a measure for nonperturbative physics in QCD (at zero temperature). Subsequently, it was regarded as an order parameter for (de)confinement and used to explore the nonperturbative natures of quark gluon plasma (QGP) [24–27]. Moreover, lattice results show that the gluon condensate is non-zero at high temperature, in particular, its value drastically changes near T_c (the critical temperature of the deconfinement transition) regardless of the number of quark flavors [28]. Due to the above reasons, it would be natural and very interesting to study the possible effect that the gluon condensate might cause on various observables or quantities. Recently, there has been such research from holography. For instance, the effect of the gluon condensate on the heavy quark potential was studied in [29] and it was shown that the potential becomes deeper as the value of the gluon condensate decreases. Also, the gluon condensate dependence of the jet quenching parameter and drag force was considered in [30] and it was found that the inclusion of the gluon condensate increases the energy loss. Not long ago, the authors of [31] analyzed the effect of the gluon condensate on the imaginary potential and found the dropping gluon condensate reduces the absolute value of imaginary potential thus decreasing the thermal width. Motivated by this, in this paper we study the effect of the gluon condensate on the Schwinger effect. More immediately, we want to understand how the gluon condensate affects the production rate. Also, this work could be considered as the generalization of [7] to the case with gluon condensation.

The organization of the paper is as follows. In the next section, we introduce the deformed AdS backgrounds with backreaction due to the gluon condensate. In section 3, we perform the potential analysis for the Schwinger effect in these backgrounds and discuss how the gluon condensate modifies the production rate. The conclusions and discussions are given in section 4.

II. SETUP

The 5-dimensional (5D) gravity action (in Minkowski) with a dilaton coupled is given by [32]

$$I = \frac{1}{2\kappa^2} \int d^5x \sqrt{g} (\mathcal{R} + \frac{12}{R^2} - \frac{1}{2} \partial_M \phi \partial^M \phi), \quad (4)$$

where κ^2 is the 5D Newtonian constant. \mathcal{R} denotes the Ricci scalar. R represents the AdS curvature (hereafter we set $R = 1$). ϕ refers to the dilaton, coupled to the gluon operator. By solving the Einstein equation and the dilaton equation of motion, one can obtain two relevant solutions. The first is the dilaton-wall solution, given by [33, 34]

$$ds^2 = r^2 \sqrt{1 - c^2 r^{-8}} (d\vec{x}^2 - dt^2) + \frac{dr^2}{r^2}, \quad (5)$$

and the corresponding dilaton profile is

$$\phi(r) = \sqrt{\frac{3}{2}} \log\left(\frac{1 + cr^{-4}}{1 - cr^{-4}}\right) + \phi_0, \quad (6)$$

where $\vec{x} = x_1, x_2, x_3$ are the boundary coordinates. r describes the 5D coordinate and the boundary is $r = \infty$. ϕ_0 denotes a constant. c represents the gluon condensation.

Another is the dilaton black hole solution, given by [35, 36]

$$ds^2 = r^2 H(r) d\vec{x}^2 - r^2 P(r) dt^2 + \frac{dr^2}{r^2}, \quad (7)$$

with

$$\begin{aligned} H(r) &= (1 + fr^{-4})^{(f+a)/2f} (1 - fr^{-4})^{(f-a)/2f}, \\ P(r) &= (1 + fr^{-4})^{(f-3a)/2f} (1 - fr^{-4})^{(f+3a)/2f}, \\ f^2 &= a^2 + c^2, \end{aligned} \quad (8)$$

and

$$\phi(r) = \frac{c}{f} \sqrt{\frac{3}{2}} \log\left(\frac{1 + fr^{-4}}{1 - fr^{-4}}\right) + \phi_0. \quad (9)$$

As discussed in [36], the solution (7) is well defined only in the range $r_f < r < \infty$ with $r_f \equiv f^{1/4}$, where r_f could be considered as the IR cut-off. The parameter f determines the position of the singularity. a is related to the temperature as $a = (\pi T)^4/4$. Note that for $a = 0$, (7) reduces to the dilaton-wall solution, and for $c = 0$ it becomes the Schwarzschild black hole solution. Moreover, there is a Hawking-Page transition between (5) and (7) at some critical value of a . Therefore, the dilaton-wall solution is for the confined phase and the dilaton black hole solution is for the deconfined phase. For more details about the two solutions, we refer to [36].

III. POTENTIAL ANALYSIS IN SCHWINGER EFFECT

In this section we follow the approach in [7] to study the effect of the gluon condensate on the Schwinger effect. Since the dilaton-wall background could be derived from the dilaton black hole background by plugging $a = 0$ in (7), we will perform (only) the potential analysis for the latter but discuss the results for both.

A. Coulomb potential and static energy

One considers a rectangular Wilson loop on the probe D3-brane located at $r = r_0$ and impose the following ansatz

$$t = \tau, \quad x_1 = \sigma, \quad x_2 = 0, \quad x_3 = 0, \quad r = r(\sigma). \quad (10)$$

The Nambu-Goto action is

$$S = T_F \int d\tau d\sigma \mathcal{L} = T_F \int d\tau d\sigma \sqrt{g}, \quad T_F = \frac{1}{2\pi\alpha'} \quad (11)$$

where T_F denotes the string tension. α' is related to λ by $\frac{R^2}{\alpha'} = \frac{1}{\alpha'} = \sqrt{\lambda}$. g denotes the determinant of the induced metric with

$$g_{\alpha\beta} = g_{\mu\nu} \frac{\partial X^\mu}{\partial \sigma^\alpha} \frac{\partial X^\nu}{\partial \sigma^\beta}, \quad (12)$$

where $g_{\mu\nu}$ and X^μ are the metric and target space coordinates, respectively.

Plugging (10) into (7), the Lagrangian reads

$$\mathcal{L} = \sqrt{A(r) + B(r)\left(\frac{dr}{d\sigma}\right)^2}, \quad (13)$$

with

$$A(r) = r^4 H(r) P(r) e^{\phi(r)}, \quad B(r) = P(r) e^{\phi(r)}. \quad (14)$$

Since \mathcal{L} does not depend on σ explicitly, the corresponding Hamiltonian is a constant

$$\mathcal{H} = \mathcal{L} - \frac{\partial \mathcal{L}}{\partial \left(\frac{dr}{d\sigma}\right)} \left(\frac{dr}{d\sigma}\right) = \text{Constant}. \quad (15)$$

Imposing the boundary condition at $\sigma = 0$,

$$\frac{dr}{d\sigma} = 0, \quad r = r_c \quad (r_f < r_c < r_0), \quad (16)$$

given that, one has

$$\frac{dr}{d\sigma} = \sqrt{\frac{A^2(r) - A(r)A(r_c)}{A(r_c)B(r)}}, \quad (17)$$

where $A(r_c) = A(r)|_{r=r_c}$.

Integrating (17), the inter-distance between the $q\bar{q}$ (test particles) can be written as

$$x = 2 \int_{r_c}^{r_0} dr \sqrt{\frac{A(r_c)B(r)}{A^2(r) - A(r)A(r_c)}}. \quad (18)$$

On the other hand, plugging (13) and (17) into (11), the sum of Coulomb potential and static energy of the $q\bar{q}$ is expressed as

$$V_{CP+E} = 2T_F \int_{r_c}^{r_0} dr \sqrt{\frac{A(r)B(r)}{A(r) - A(r_c)}}. \quad (19)$$

B. critical electric field

Next, we calculate the critical field. The DBI action takes the form

$$S_{DBI} = -T_{D3} \int d^4x \sqrt{-\det(G_{\mu\nu} + \mathcal{F}_{\mu\nu})}, \quad (20)$$

where

$$T_{D3} = \frac{1}{g_s(2\pi)^3\alpha'^2}, \quad \mathcal{F}_{\mu\nu} = 2\pi\alpha' F_{\mu\nu}, \quad (21)$$

with T_{D3} the D3-brane tension.

Applying (7) and assuming the electric field is turned on along the x_1 -direction [7], one has

$$G_{\mu\nu} + \mathcal{F}_{\mu\nu} = \begin{pmatrix} -r^2 P(r) e^{\phi(r)/2} & 2\pi\alpha' E & 0 & 0 \\ -2\pi\alpha' E & r^2 H(r) e^{\phi(r)/2} & 0 & 0 \\ 0 & 0 & r^2 H(r) e^{\phi(r)/2} & 0 \\ 0 & 0 & 0 & r^2 H(r) e^{\phi(r)/2} \end{pmatrix}, \quad (22)$$

which gives

$$\det(G_{\mu\nu} + \mathcal{F}_{\mu\nu}) = r^4 H^2(r) e^{\phi(r)} [(2\pi\alpha')^2 E^2 - r^4 P(r) H(r) e^{\phi(r)}]. \quad (23)$$

Putting (23) into (20) and making the D3-brane located at $r = r_0$, one obtains

$$S_{DBI} = -T_{D3} r_0^2 H(r_0) e^{\phi(r_0)/2} \int d^4x \sqrt{r_0^4 P(r_0) H(r_0) e^{\phi(r_0)} - (2\pi\alpha')^2 E^2}, \quad (24)$$

where $P(r_0) = P(r)|_{r=r_0}$, etc.

The quantity under the square root of (24) should be non-negative, yielding

$$r_0^4 P(r_0) H(r_0) e^{\phi(r_0)} - (2\pi\alpha')^2 E^2 \geq 0, \quad (25)$$

resulting in

$$E \leq \frac{1}{2\pi\alpha'} r_0^2 \sqrt{P(r_0) H(r_0) e^{\phi(r_0)}} \equiv T_F r_0^2 \sqrt{P(r_0) H(r_0) e^{\phi(r_0)}}. \quad (26)$$

At last, one arrives at the critical field

$$E_c = T_F r_0^2 \sqrt{P(r_0) H(r_0) e^{\phi(r_0)}}, \quad (27)$$

one can see that E_c depends on the temperature as well as the gluon condensate.

C. total potential

The remaining task is to compute the total potential, which takes the form

$$\begin{aligned}
V_{tot}(x) &= V_{CP+E} - Ex \\
&= 2T_F \int_{r_c}^{r_0} dr \sqrt{\frac{A(r)B(r)}{A(r) - A(r_c)}} \\
&\quad - 2\alpha T_F r_0^2 \sqrt{P(r_0)H(r_0)e^{\phi(r_0)}} \int_{r_c}^{r_0} dr \sqrt{\frac{A(r_c)B(r)}{A^2(r) - A(r)A(r_c)}}.
\end{aligned} \tag{28}$$

where $\alpha \equiv \frac{E}{E_c}$. It seems quite difficult to evaluate the above expression analytically, but it is possible numerically. To ensure stable numerics, it turns out to be more convenient to use the following dimensionless parameters like

$$y \equiv \frac{r}{r_c}, \quad m \equiv \frac{r_c}{r_0}, \tag{29}$$

given that, (28) becomes

$$\begin{aligned}
V_{tot}(x) &= V_{CP+E} - Ex \\
&= 2T_F m r_0 \int_1^{1/m} dy \sqrt{\frac{A(y)B(y)}{A(y) - A(y_c)}} \\
&\quad - 2\alpha T_F m r_0^3 \sqrt{P(r_0)H(r_0)e^{\phi(r_0)}} \int_1^{1/m} dy \sqrt{\frac{A(y_c)B(y)}{A^2(y) - A(y)A(y_c)}}.
\end{aligned} \tag{30}$$

where

$$\begin{aligned}
A(y) &= (mr_0 y)^4 H(y) P(y) e^{\phi(y)}, & A(y_c) &= (mr_0)^4 H(y_0) P(y_0) e^{\phi(y_0)}, \\
B(y) &= P(y) e^{\phi(y)}, & \phi(y) &= \frac{c}{f} \sqrt{\frac{3}{2}} \log\left(\frac{1 + f(mr_0 y)^{-4}}{1 - f(mr_0 y)^{-4}}\right) + \phi_0, \\
H(y) &= (1 + f(mr_0 y)^{-4})^{\frac{f+a}{2f}} (1 - f(mr_0 y)^{-4})^{\frac{f-a}{2f}}, \\
P(y) &= (1 + f(mr_0 y)^{-4})^{\frac{f-3a}{2f}} (1 - f(mr_0 y)^{-4})^{\frac{f+3a}{2f}},
\end{aligned} \tag{31}$$

with $H(y_0) \equiv H(r)|_{r=mr_0}$, $P(y_0) \equiv P(r)|_{r=mr_0}$ and $\phi(mr_0) \equiv \phi(r)|_{r=mr_0}$. One can check that by turning off the gluon condensate effect in (30), the results of SYM case [7] are recovered (note that the temperature formula in this paper without gluon condensate is $r_f = \pi T/\sqrt{2}$ but that in [7] is $r_h = \pi T$).

D. dilaton-wall result

Before numerical computation, we determine the values of some parameters. First, we set $T_F = 1$ and choose an appropriate value of r_0 , e.g., $r_0 = 3$, similar to [7]. Also, we take $0 \leq c \leq 0.9 GeV^4$ and $\phi_0 = 0$, as follows from [29, 30].

We first discuss the results for the dilaton-wall background (zero temperature case). In fig.1, we plot $V_{tot}(x)$ against x with different values of c , where the left panel is for $c = 0.02 GeV^4$ (small gluon condensate) while the right one $c = 0.9 GeV^4$ (large gluon condensate). Other cases with different values of c have similar picture. From these figures, one can see that there are mainly three situations: When $E < E_c$ ($\alpha < 1$), the potential barrier is present and the Schwinger effect can occur as a tunneling process. As E increases, the potential barrier decreases gradually and vanishes at $E = E_c$ ($\alpha = 1$). When $E > E_c$ ($\alpha > 1$), the system becomes catastrophically unstable. The above analysis are in agreement with [7].

In order to study how the gluon condensate influences the Schwinger effect, we plot $V_{tot}(x)$ versus x with fixed $\alpha = 0.8$ for different values of c in the left panel of fig.2. One can see that as c increases, the height and width of the potential barrier both increase. As you know, the higher (or the wider) the potential barrier, the harder the produced pair escapes to infinity. Therefore, one concludes that the presence of the gluon condensate increases the potential barrier thus decreasing the Schwinger effect.

Also, one can analyze the effect of the gluon condensate on the critical field. To this end, we plot E_c versus c in the right panel of fig.2. One finds that increases c leads to increasing E_c thus making the Schwinger effect harder, consistently the previous potential analysis.

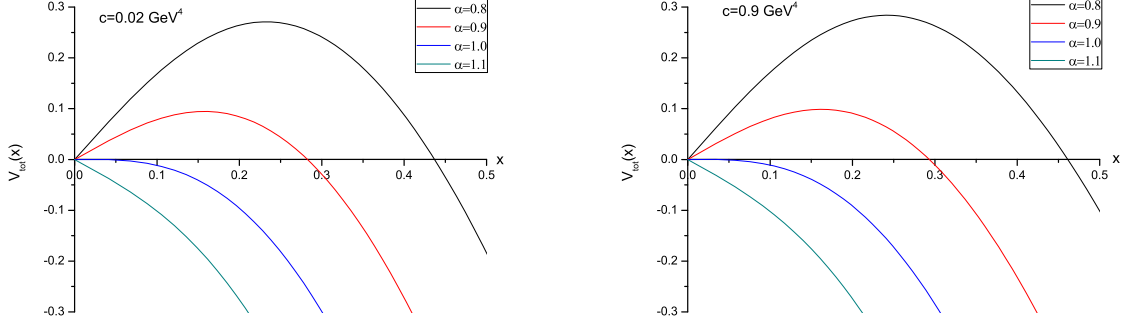


FIG. 1: $V_{tot}(x)$ versus x with different c for the dilaton-wall background. In both panels from top to bottom $\alpha = 0.8, 0.9, 1.0, 1.1$, respectively.

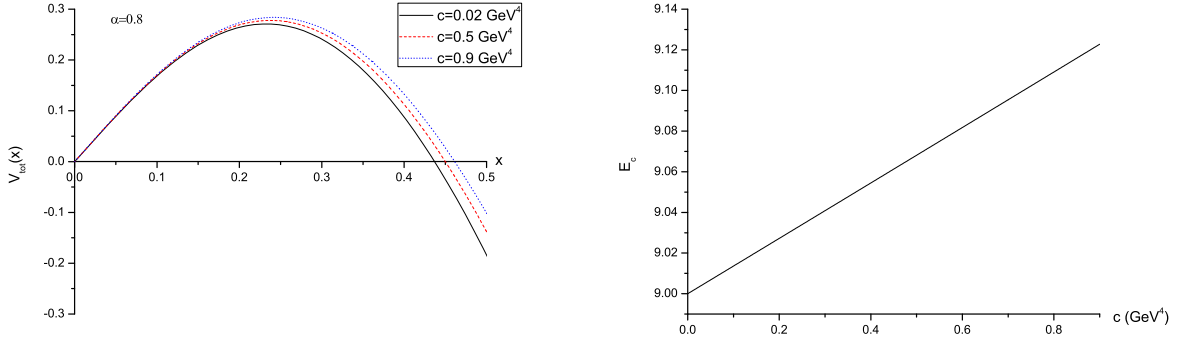


FIG. 2: Left: $V_{tot}(x)$ versus x with fixed $\alpha = 0.8$ and different c for the dilaton-wall background. From top to bottom $c = 0.9, 0.5, 0.02 \text{ GeV}^4$, respectively. Right: E_c versus c .

E. dilaton black hole result

Next, we discuss the results for the dilaton black hole background (finite temperature case). Likewise, the findings are presented in form of plots, i.e., fig.3~fig.5, where fig.3 shows the general behavior of the potential for various T and fixed c (other cases with different values of c have similar picture). One can see that there are still three cases for the potential, similar to the dilaton-wall case.

In order to see how the gluon condensate modifies the Schwinger effect at non-zero temperature, we plot $V_{tot}(x)$ versus x with fixed T and different values of c in the left panel of fig.4. One gets similar results: the inclusion of the gluon condensate increases the potential barrier thus decreasing the Schwinger effect. Also, the same conclusion could be obtained from the gluon condensate dependence of E_c (see the right panel of fig.4): E_c increases with c . Interestingly, it was argued [13] that the D-instanton density (corresponds to the vacuum expectation value of the gluon condensation) decreases the Schwinger effect as well.

Furthermore, to understand the temperature dependence of the Schwinger effect, we plot $V_{tot}(x)$ versus x with different T (as well as E_c versus T) in fig.5. From the left panel, one can see that at fixed c , increasing T leads to decreasing the potential barrier, while from the right panel one finds E_c decreases with T , which means increasing T enhances the Schwinger effect. Therefore, the gluon condensate and temperature have opposite effects on the Schwinger effect. The physical significance of the results will be discussed in the next section

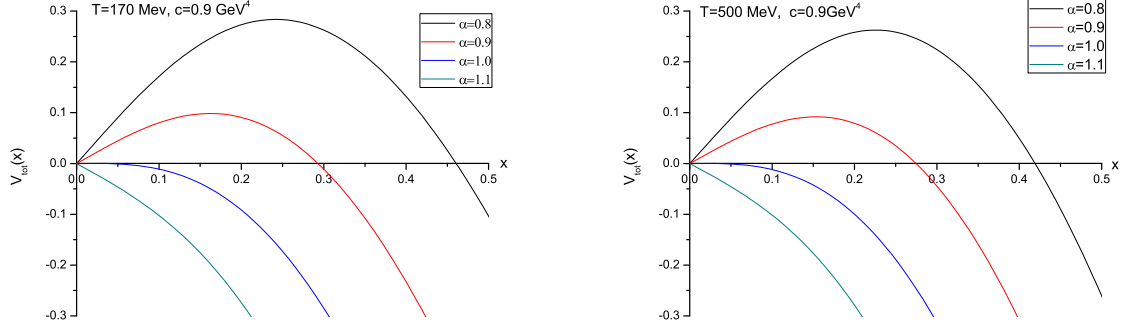


FIG. 3: $V_{tot}(x)$ versus x with fixed $c = 0.9 \text{ GeV}^4$ and different T for the dilaton black hole background. Left: $T = 170 \text{ MeV}$; Right: $T = 500 \text{ MeV}$. In both panels from top to bottom $\alpha = 0.8, 0.9, 1.0, 1.1$, respectively.

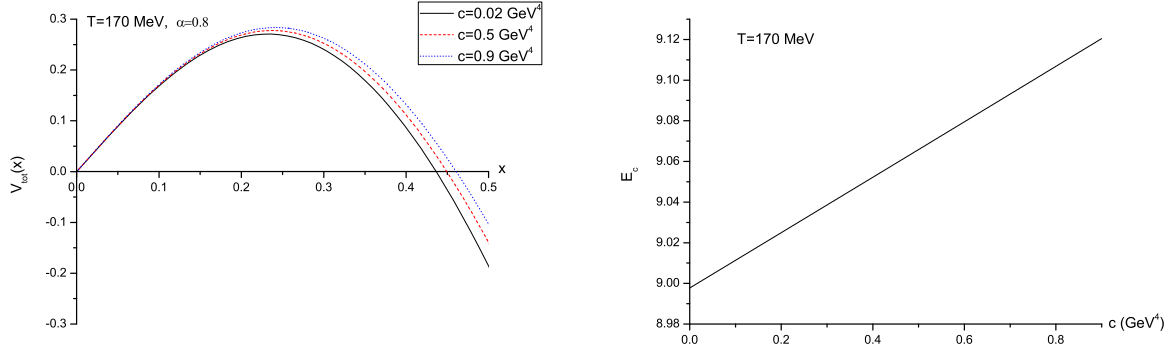


FIG. 4: Left: $V_{tot}(x)$ versus x with fixed $\alpha = 0.8$, $T = 170 \text{ MeV}$ and different c for the dilaton black hole background. From top to bottom $c = 0.9, 0.5, 0.02 \text{ GeV}^4$, respectively. Right: E_c versus c .

IV. CONCLUSION AND DISCUSSION

In this paper, we studied the effect of the gluon condensate on the Schwinger effect in dilaton-wall background and dilaton black hole background, respectively. We evaluated the electrostatic potentials by calculating the Nambu-Goto action of a string attaching the rectangular Wilson loop on a probe D3 brane. Also, we determined E_c from the DBI action and plotted it as a functions of c for various cases. For both backgrounds, we observed that increasing c leads to increasing the potential barrier thus reducing the Schwinger effect. One step further, the presence of the gluon condensate reduces the production rate, in agreement with the finding of [13]. Also, we found the temperature has opposite effect on the Schwinger effect.

One may wonder how gluon condensate modifies the Schwinger effect in the investigated temperature ranges (in particular associated with experiment)? We would like to make the following comment. It was shown [28] that the value of c drops near the deconfinement transition. And at high temperatures, c becomes independent of T and μ (the chemical potential), but when T is not very high, c strongly depends on T and μ [37]. Taken together, one may infer that the Schwinger effect (or production rate) increases as c decreases in the deconfined phase, and almost won't be modified by c at high temperature. However, we could not give a concrete conclusion for intermediate temperature or low temperature. To resolve this problem, we need to study the competitive effects of c , μ , T (on the Schwinger effect) as well as the relationship between the three. We hope to report our progress in this regard in the near future.

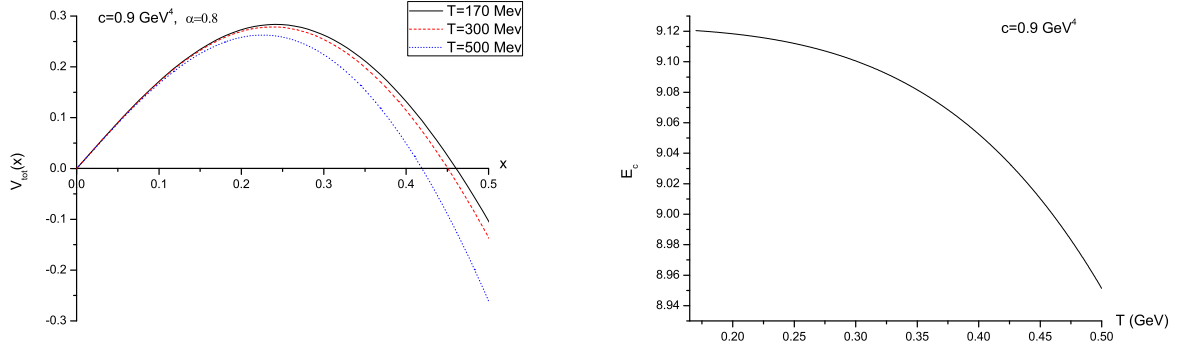


FIG. 5: Left: $V_{tot}(x)$ versus x with fixed $\alpha = 0.8$, $c = 0.9 \text{ GeV}^4$ and different c for the dilaton black hole background. From top to bottom $T = 170, 300, 500 \text{ MeV}$, respectively. Right: E_c versus T .

V. ACKNOWLEDGMENTS

This work is supported by the NSFC under Grant Nos. 11735007, 11705166 and the Fundamental Research Funds for the Central Universities, China University of Geosciences (Wuhan) (No. CUGL180402). The work of Xiangrong Zhu is supported by Zhejiang Provincial Natural Science Foundation of China No. LY19A050001.

-
- [1] J. S. Schwinger, Phys. Rev. 82 (1951) 664.
 - [2] I. K. Affleck and N. S. Manton, Nucl. Phys. B 194 (1982) 38.
 - [3] J. M. Maldacena, Adv. Theor. Math. Phys. 2, 231 (1998).
 - [4] S. S. Gubser, I. R. Klebanov and A. M. Polyakov, Phys. Lett. B 428, 105 (1998).
 - [5] O. Aharony, S. S. Gubser, J. Maldacena, H. Ooguri and Y. Oz, Phys. Rept. 323, 183 (2000).
 - [6] G. W. Semenoff and K. Zarembo, Phys. Rev. Lett. 107 (2011) 171601.
 - [7] Y. Sato and K. Yoshida, JHEP 1308 (2013) 002.
 - [8] Y. Sato and K. Yoshida, JHEP 1309 (2013) 134.
 - [9] Y. Sato and K. Yoshida, JHEP 1312 (2013) 051.
 - [10] K. B. Fadafan and F. Saiedi, Eur.Phys.J. C (2015) 75:612.
 - [11] M. Ghodrati, Phys. Rev. D 92, 065015 (2015).
 - [12] Z. q. Zhang, Nucl. Phys. B 935 (2018) 377.
 - [13] L. Shahkarami, M. Dehghani, P. Dehghani, Phys. Rev. D 97, 046013 (2018).
 - [14] S. Chakraborty and B. Sathiapalan, Nucl.Phys. B 890 (2014) 241.
 - [15] S. Bolognesi, F. Kiefer, E. Rabinovici, JHEP 1301, 174 (2013).
 - [16] Y. Sato, K. Yoshida, JHEP 1304, 111 (2013).
 - [17] W. Fischler, P.H. Nguyen, J.F. Pedraza, W. Tangarife, Phys. Rev. D 91, 086015 (2015).
 - [18] K. Hashimoto and T. Oka, JHEP 1310 (2013) 116.
 - [19] K. Hashimoto, T. Oka, and A. Sonoda, JHEP 1406 (2014) 085.
 - [20] X. Wu, JHEP 09 (2015) 044.
 - [21] K. Ghoroku, M. Ishihara, JHEP 09 (2016) 011.
 - [22] D. Kawai, Y. Sato, and K. Yoshida, Int.J.Mod.Phys. A 30 (2015) 1530026.
 - [23] M. A. Shifman, A.I. Vainshtein and V.I. Zakharov, Nucl. Phys. B 147 (1979) 385.
 - [24] S. H. Lee, Phys. Rev. D 40 (1989) 2484.
 - [25] M. D. Elia, A. D. Giacomo and E. Meggiolaro, Phys. Rev. D 67 (2003) 114504.
 - [26] D. E. Miller, Phys. Rept. 443 (2007) 55.
 - [27] G. E. Brown, J.W. Holt, C.-H. Lee and M. Rho, Phys. Rept. 439 (2007) 161.
 - [28] G. Boyd et al., Nucl. Phys. B 469, 419 (1996).
 - [29] Y. Kim, B.-H. Lee, C. Park and S.-J. Sin, Phys. Rev. D 80, 105016 (2009).
 - [30] Z. q. Zhang and X. R. Zhu, Eur. Phys. J. C (2019) 79:107.
 - [31] Y. Q. Zhao, Z. R. Zhu, X. Chen, arXiv:1909.04994.
 - [32] S. Nojiri and S.D. Odintsov, Phys. Lett. B 449 39 (1999).
 - [33] A. Kehagias and K. Sfetsos, Phys. Lett. B 454 270 (1999).

- [34] C. Csaki and M. Reece, JHEP 05 (2007) 062.
- [35] D. Bak, M. Gutperle, S. Hirano, and N. Ohta, Phys. Rev. D 70, 086004 (2004).
- [36] Y. Kim, B.-H. Lee, C. Park and S.-J. Sin, JHEP 09 (2007) 105.
- [37] P. Colangelo, F. Giannuzzi, S. Nicotri, and F. Zuo, Phys. Rev. D 88, 115011 (2013).